Population-level encoding of somatosensation in mouse sensorimotor cortex

Seungbin Park,[a,1] Megan H. Lipton,[b,1] Maria C. Dadarlat,[a]

*a*Weldon School of Biomedical Engineering, Purdue University, West Lafayette, IN
*b*Purdue University Interdisciplinary Life Science Program, Purdue University, West Lafayette, IN
1, equal contribution by the authors

1 Abstract

Dexterous limb movements rely on somatosensation (touch and proprioception), which provides the sense of the body's posture, movement, and interaction with objects. The heterogeneous responses of single neurons in sensorimotor cortex to somatosensation have led to disparate views of the computational role of this brain area in somatosensory processing. Here, we use population-level analyses of neural activity recorded during active and passive limb movements to assess the structure and summarize the properties of neural encoding in sensorimotor cortex. We used 2-photon imaging to record the activity of thousands of neurons in these brain areas from eight anesthetized mice during passive deflections of each limb. We additionally analyzed neural responses to passive limb movements in eight awake mice, sourced from an open dataset [1], and neural responses to spontaneous limb movements in eight mice, collected during a previous study [2]. To conduct the population-level analyses, we found the principal components of the time-varying neural population activity matrix in each set of experiments. Across all three datasets and behavioral conditions, a small fraction of principal components explained a large fraction of variance in the neural responses. These low-dimensional representations of single and multi-limb movements were well conserved across animals, including orthogonal representations of ipsilateral and contralateral limbs. This organization of somatosensory information mirrors the well-known structure of neural encoding of motor commands. Furthermore, while the activity of individual neurons and small populations best encoded intrinsic variables, larger populations of neurons additionally encode extrinsic variables — a representational structure that is commonly associated with higher-level brain areas. Together, these analyses demonstrate that population-level encoding of somatosensory information in mouse sensorimotor cortex is structured to facilitate sensorimotor integration across the brain.

2 Introduction

Somatosensation, including proprioception and touch, is essential for controlling fine movements [3, 4, 5, 6]. Tactile information guides object manipulation, providing information about contact location, pressure, and timing [4, 7, 5]. Proprioception is the sense of the body's position and movement through space and emerges from sensors embedded in the muscles and joints (reviewed in [6]). Proprioception is required to coordinate complex multi-joint and multi-limb movements, such as playing an instrument, where visual feedback alone is insufficient for precision and accuracy [8, 9, 10, 11, 12, 13].

The neural basis of proprioception may be studied by recording neural activity during externally-imposed perturbations (passive limb movements) in which the animal does not actively control its limb position [6, 14, 1]. Within the primary somatosensory cortex, neurons that respond to movements of the limb are tuned to both the direction and distance of movement, suggesting encoding of extrinsic variables [15, 16, 1]. However, neural activity also correlates with limb position, speed, movement amplitude, and the phase of the limb stance/swing cycle during locomotion [15, 17, 18, 1, 19]. Such variability in neural responses across behavioral tasks supports the argument that neurons are encoding whole-limb kinematics, including the configurations of multiple joints in the arm and hand –

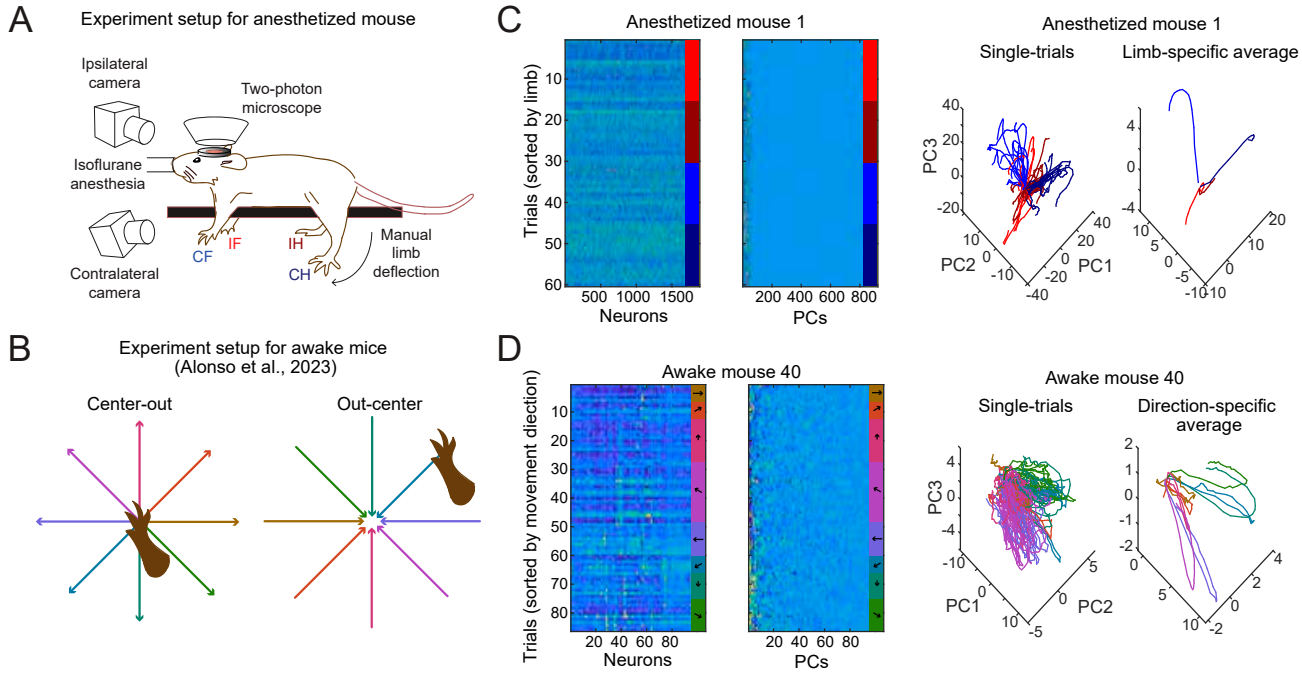

Figure 1: Experiment setup and neural representations in PC space. **A** Experimental setup for recording neural responses to limb deflection in mice anesthetized with 1-2% isoflurane in oxygen. **B** Schematic showing center-out and out-center passive planar movements in [1]. Notably, the same movement vectors (relative start and end points) are repeated with different start and end points in the two conditions. **C** A comparison of single-neuron and PCA representations of population-level activity during limb deflection in a single anesthetized mouse. At left: Z-scored single-neuron responses and PCA to limb deflection, averaged across time within each trial. Colors scale of neural responses ranges from [-1,2]. Trials were sorted by limb, shown by the colored bar on the far right of the image. Colors as in (A). At right: low-dimensional representation of time-varying neural activity, shown both for individual trials and trial averages for each limb. **D** As in (C), conducted in a single awake mouse. Colors as in (B). At right: as in (C) but trial averages for each direction.

information that is derived from the activity of muscle spindles in the limb [20, 21, 14, 22]. However, even within a fixed behavioral task, there is significant variability in the responses of single neurons within a population, prohibiting a conclusive statement regarding the "information" encoded by somatosensory cortex. Addressing this question is important to understand sensory-guided movements given the clear role that proprioception plays in movement planning and execution [9, 23, 24, 25].

Instead of examining single neurons, we propose to "summarize" the information encoded by a brain area by using population-level analysis of neural activity patterns [26, 27]. Population-level neural activity can be captured by projecting the activity of neurons into a lower-dimensional space via some form of dimensionality reduction [28, 29]. Analyzing neural activity patterns during behavior in this low-dimensional "state space" has been pivotal for understanding cortical encoding of vision, olfaction, and motor planning as well as for understanding thalamic encoding of somatosensation [30, 28, 31, 32, 33]. In the mouse, somatosensory information from the forelimb is distributed across both somatosensory and motor cortices [1]. We therefore hypothesized that analyzing the low-dimensional representations of somatosensation in mouse sensorimotor cortex may elucidate the neural structure and thus function of these brain areas.

Analyzing the low-dimensional representation of neural encoding of somatosensation also facilitates a direct comparison to the known structure of neural encoding of motor commands [33]. From the perspective of sensorimotor integration, sensory and motor signals must be combined for sensory information to guide movements; before this can happen, however, sensory and motor signals must be

converted into a common reference frame [24]. Applying a state-space perspective to neural encoding of somatosensation offers a rather literal way to compare these reference frames [34]. For example, neural population activity within motor cortex during reaching is well described as a low-dimensional dynamical system, where the rate of change of a neural population's activity is a function of ongoing neural activity and external input [33, 35, 36, 17]. However, the dimensionality of somatosensory information in the cortex is unknown. Furthermore, state-space encoding of ipsilateral and contralateral limbs during active movements are orthogonal in motor cortex.[37, 38, 39]. While sensorimotor cortex shows clear responses to ipsilateral limbs, the activity patterns of single neurons relative to their responses to contralateral limbs are highly variable [40]. Analyzing the low-dimensional representation of ipsilateral and contralateral limbs in mouse sensorimotor cortex may clarify their computational role in this brain area. Directly addressing these questions will yield insight into the neural processes underlying sensorimotor integration — the closed-loop process by which humans and animals use sensory information to guide movements.

In this manuscript we use principal component analysis (PCA) to "summarize" activity within a large population of neurons recorded from mouse sensorimotor cortex in both anesthetized and awake mice. Using low-dimensional representations, we found that the structure of neural activity in mouse sensorimotor cortex that arises from somatosensory inputs from the limbs mirrors the observed low-dimensional structure of motor commands. These representations were well-conserved across animals and could demonstrate that correlated activity across neural populations can encode sensory variables that differ from single neuron representations. Together, our results illustrate how the parallel structure of somatosensation and motor commands may facilitate sensorimotor integration across the brain.

3 Results

In this study we examined population-level neural encoding of limb movements in mouse sensorimotor cortex in three contexts: 1) during passive deflections of each of the four limbs of anesthetized mice (Figure 1A) during passive movements of a single forelimb contralateral to the cortical hemisphere in which neural signals were recorded (using an open-source dataset [1]; Figure 1B), and 3) during spontaneous movements in head-fixed freely-moving mice (which we previously published [41, 42]). These complementary datasets each offer unique insights into neural encoding of somatosensation. In all three datasets, neural activity was recorded with two-photon calcium imaging.

3.1 Low-dimensional encoding of limb movements in mouse sensorimotor cortex

We first calculated the dimensionality of neural activity within mouse sensorimotor cortex. Given the low dimensionality of activity patterns in somatosensory thalamus and motor cortex during active movements [28, 33], a straightforward prediction is that encoding of somatosensation in sensorimotor cortex would be similarly low-dimensional. However, the significant anatomical expansion from the thalamus to the cortex could mediate a corresponding increase in the dimensionality of somatosensory encoding that serves to enhance the discriminability of stimuli [43, 44, 45].

To test this idea, we found the principal components of the neural responses to passive and active limb movements (see Methods: Principal component analysis (PCA) and dimensionality analysis). Plotting the neural response matrix in PC space clearly shows that neural activity is highly correlated and thus concentrated in a fraction of the total possible dimensions (Figure 1C,D, left panels). We observed distinct neural activity patterns associated with passive movements of each limb and with movements of a single limb to different directions (Figure 1C,D, right panels). To calculate the dimensionality of neural activity, we found the number of significant PCs within the datasets. The dimensionality of the neural response matrix was taken to be the number of eigenvalues that were significantly larger than the largest eigenvalue found for a set of randomly-permuted data matrices.

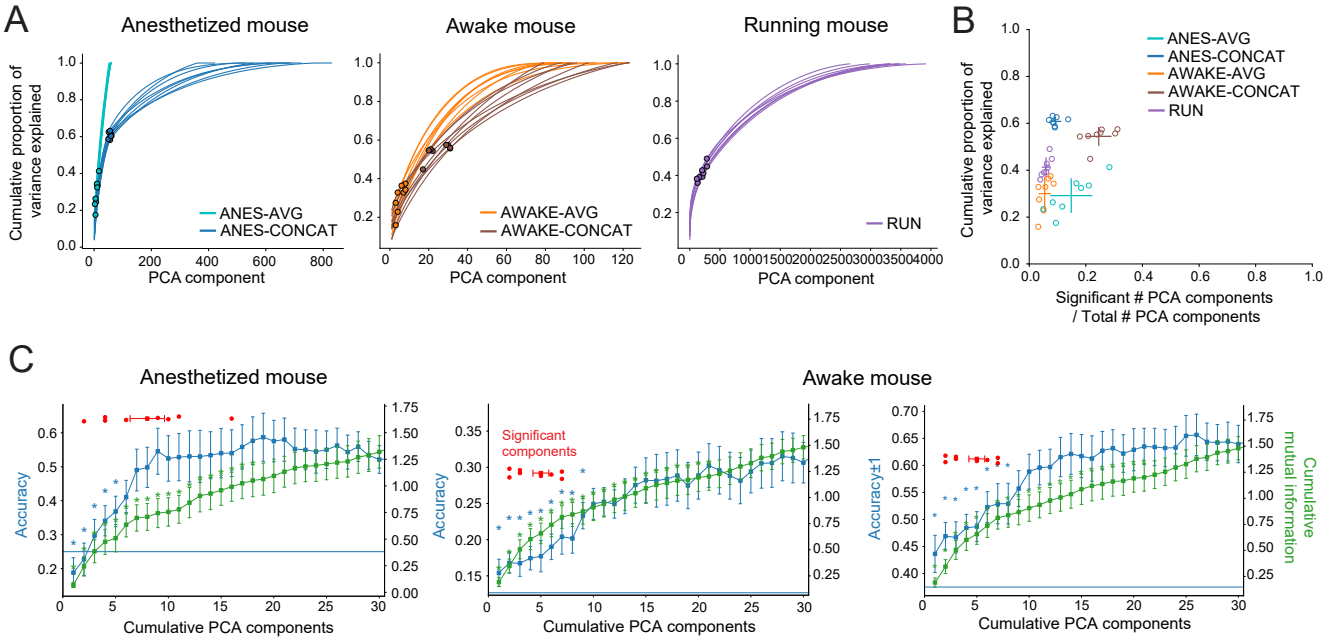

Figure 2: Dimensionality of neural representation of somatosensation in anesthetized, awake, and running animals. **A** Cumulative proportion of variance explained by principal components obtained from the average across trials from anesthetized animals (ANES-AVG), the trial-concatenated from anesthetized animals (ANES-CONCAT), the average across trials from awake animals (AWAKE-AVG), the trial-concatenated from awake animals (AWAKE-CONCAT), and neural responses from the running animals (RUN). Each line represents the result from an animal where a circle shows the significant PC. **B** Cumulative proportion of variance explained of the ratio between the number of the significant PCs and the total number of PCs. **C** Accuracy of decoding target limbs for the anesthetized mice (left) and angles of passive proprioceptive stimuli for the awake mice (middle and right) using cumulative principal components and the cumulative mutual information between each PC and sensory variables. Horizontal lines show chance levels. Red dots show the obtained significant PCs of all animals, with the mean in the squared and error bars. Wilcoxon rank-sum test was performed to compare the score of each component and the maximum.

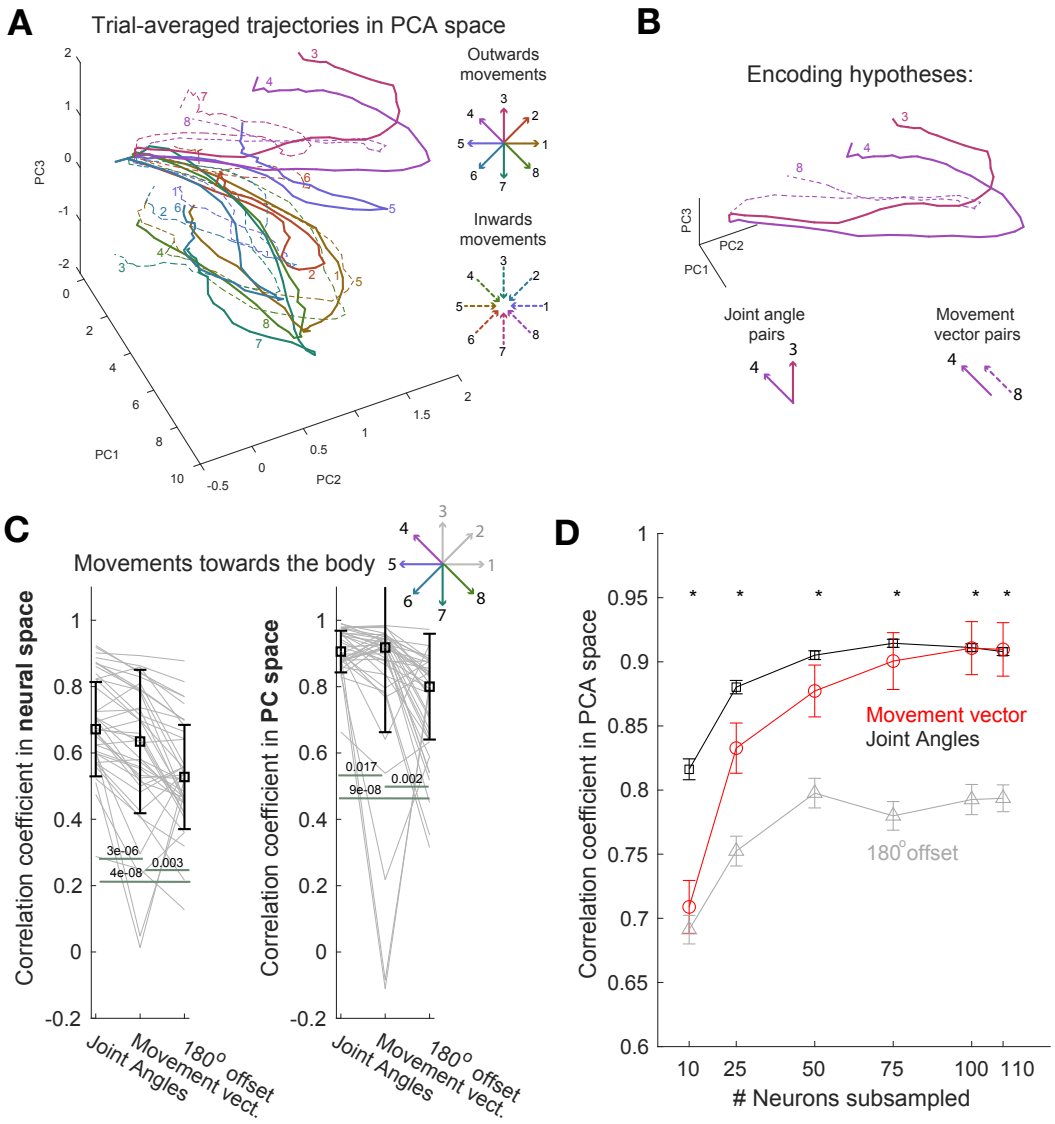

Figure 3: Population-level encoding of passive limb movements in neural space and PC space. **A** Trial-averaged neural responses to each movement direction during outwards and inwards movements projected onto PC space. Responses are shown along the first three PCs. Colors match movement vector pairs between the outwards and inward movements. **B** Graphical illustration of our test of two competing sensory encoding hypotheses. If the neural population encodes joint angles rather than movement vectors, the neural trajectories for joint angle pairs will be more correlated than movement trajectories for movement vector pairs. **C** Correlation between neural trajectories corresponding to pairs of movements. Neural data from mice with at least 75 simultaneously recorded neurons (n = 8) was analyzed, during movement in directions 4-8 (shown in the upper right). "Joint angles" compares trajectories for movements with 45° separation for outwards movement data. It includes the value for the closest of two possible neighbors (e.g., movement 4 could be more similar to movement 3 or to movement 5). "Movement vect." compares trajectories for the same movement vectors during outwards and inwards movement. "180° offset" compares trajectories for movement in opposite directions during outwards movements, and functions as a control for the two hypotheses. Correlations are computed for multi-dimensional data using all of the neurons (neural space) or along the first five PCs (PC space). Significance between groups is calculated using a Wilcoxon rank-sum test. **D** Analysis as in (C), repeated using sub-samples of the total neural population to compute PCs (restricted to animals with at least 110 neurons recorded simultaneously, N = 3). Significance between groups is calculated using a Wilcoxon rank-sum test.

To compare across datasets with different numbers of neurons, the number of significant PCs was then normalized by the total number of independent variables to eliminate the effect of the size of the data on the significant PCs (see Methods: Principal component analysis (PCA) and dimensionality analysis; [46]). Based on this analysis, we find that the number of significant PCs makes up only a small fraction of the total number of variables (neurons) included in the analysis (below 0.2). However, this small number of significant principal components explained a large fraction of variance (0.3–0.6 cumulative proportion of variance explained; Figure 2A,B and Tables S1-3). The ratio of the fraction of significant components to cumulative variance explained is highly conserved both across animals and across the anesthetized/awake/running datasets, despite both the difference in task structure in the datasets and the variability in the number of neurons recorded in each animal. Furthermore, these results are consistent with past work evaluating the dimensionality of neural activity across the brain involved in sensory and motor function but also in memory and cognition [47], suggesting that we are capturing a general feature of neural encoding.

Quantifying the dimensionality of the data, however, does not directly address the information encoded by the neural population. The question is: how well does population-level neural activity encode variables describing passive limb movements? We used two metrics to answer this question: decoding accuracy and mutual information between neural responses and limb movements. For the first metric, we characterized the accuracy of a linear classifier (linear discriminant analysis) in decoding sensory variables relevant to each dataset. As we have previously shown that limb position can be decoded from neural activity in sensorimotor cortex of awake, running mice [41], we focus here on decoding sensory variables during passive movements. In the anesthetized dataset, the sensory variable was the identity of the limb being deflected. In the awake dataset, the sensory variable was the direction (angle; one of the eight that divides the horizontal plane) of movement during center-out reaches. Both sensory variables could be decoded with modest accuracy (Figure 2C). Notably, decoding accuracy plateaued (failed to significantly improve with additional components) around the average number of significant components found across animals. Cumulative mutual information between each PC and sensory variables followed a similar trend, but plateaued later. These results show that a small fraction of principal components include sufficient information to encode each sensory variables, which aligns with the idea that a small fraction of the components explain a large part of the variance explained. The results support our assertion that that neural responses to somatosensation are low-dimensional.

3.2 Intrinsic vs. extrinsic encoding of limb movements

The variability in single-neuron tuning to passive limb movements across distinct behavioral tasks has yielded mixed conclusions regarding the sensory variables encoded by somatosensory cortex [15, 20, 21, 14, 22, 1], including whether somatosensory cortex encodes proprioceptive information in terms of joint angles or as a movement vector. Joint angles refers to the specific configuration of a limb: the angle between the trunk of the body and the upper limb (the shoulder) and the angle between the upper limb and the forelimb (the elbow). In contrast, a movement vector represents the distance and direction between the start and end points of a movement. While the two variables are closely related (given the same starting point of the limb, similar movement vectors will result in similar changes in joint angles), an identical movement vector can be achieved by distinct changes in joint angles. The awake open-source dataset was designed to test this hypothesis at the level of single neurons: the mouse's forelimb was moved through the same movement vectors with two distinct starting points, generating either center-out or out-center movements (Figure 1B). They found that many single neurons often had similar responses to the same movement vector, regardless of starting point [1]. However, given the variability across single-neuron responses, it is important to additionally characterize population-level responses. To test the hypothesis that neural populations similarly encode movement vectors rather than joint angles, we used neural responses in the reference frame of principal components of the data

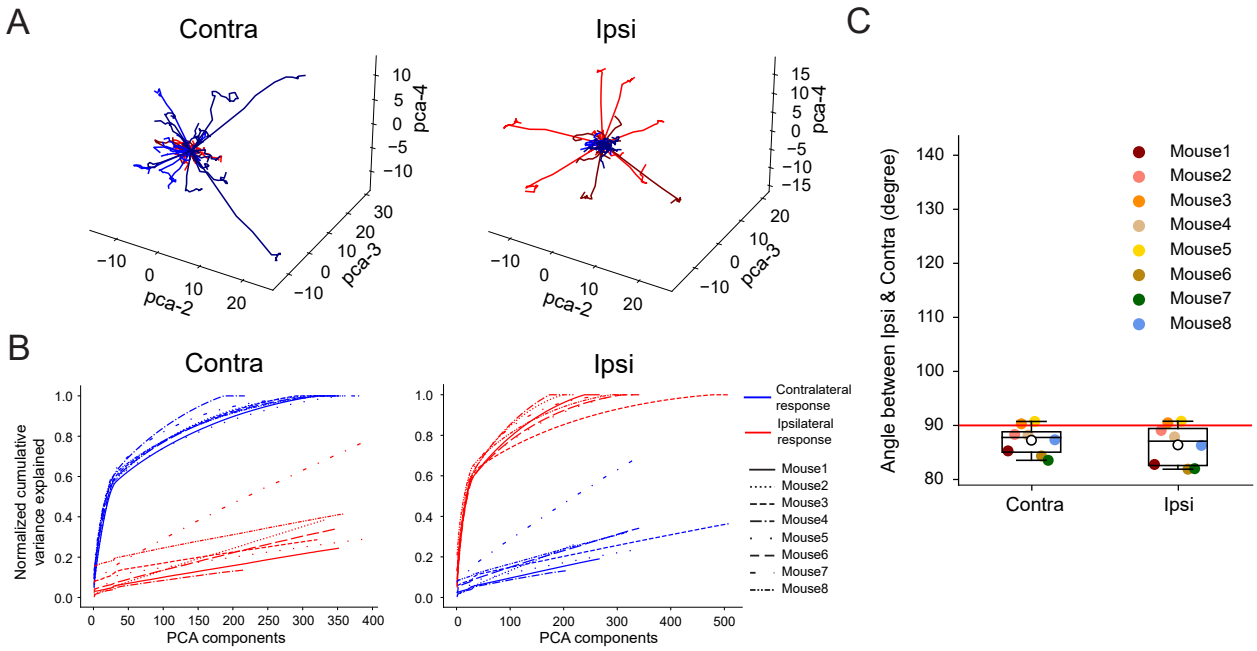

Figure 4: Orthogonality between the projections of ipsilateral and contralateral limb representations in sensorimotor cortex into different PC spaces. **A** PC projections of all trial responses onto the PC space obtained from contralateral limb responses (*Contra*) and ipsilateral limb responses (*Ipsi*). **B** Normalized cumulative variance explained of PCs in *Contra* and *Ipsi* spaces. **C** Angle between projections of ipsilateral and contralateral responses in *Contra* and *Ipsi* spaces.

to analyze population-level encoding of limb movements in the awake dataset.

Each hypothesis (joint-angle or movement-vector) makes a distinct prediction about the structure of neural responses in both neural space and in principal component space. "Neural space" refers to the set of simultaneously recorded z-score neural responses to limb movement, where each neuron defines a dimension in neural space. "PC space" refers to the neural response matrix projected onto the set of significant principal components. If the movement vector hypothesis were true, the neural representations of pairs of movement vectors (during inwards and outwards movements, which require different changes in joint angles) would be more similar than neural representations of movements in neighboring directions that had the same starting point (which require similar changes in joint angles; Figure 3B). To test this hypothesis, we first projected the neural responses to both inwards and outwards movements into a unified principal component space (Figure 3A). We then quantified the similarity between neural representations of movement pairs (joint angle pairs, movement vector pairs, or 180° offset pairs) by calculating the correlation coefficient between trial-averaged neural trajectories in PC space (Figure 3C). As a control, we also computed the similarity between each movement and its direct opposite (movements offset by 180°), which are dissimilar in terms of both changes in joint angle and in terms of movement vectors. Thus, the 180° offset provides a lower bound for similarity in this dataset. Given the established asymmetry of single-neuron tuning to movement directions [1], we restricted the analysis to movements between 135° to 315° (towards the mouse's body; see inset in Figure 3C). Furthermore, we restricted the analysis to animals with at least 75 simultaneously-recorded neurons; however, we did not exclude neurons from analysis on the basis of particular responses properties (e.g., tuning to movements).

We found that population-level activity in neural space was most consistent with encoding joint angles (Figure 3C, left panel). In contrast, population-level activity in principal component space

was most consistent with encoding of movement vectors (Figure 3C, right panel). The discrepancy in encoding results between neural and principal component spaces leads us to hypothesize that movement vector information may be extracted from a population of neurons that individually encode joint angles by taking a weighted average of individual neuron activity, which is what happens when neural activity is projected into PC space. This weighted average may marginalize out joint angle information, keeping the variable that was best described by correlated activity across the population: the movement vector.

In support of this hypothesis, we found that neural encoding in principal component space reverted to joint angles if fewer neurons were used to calculate the principal components. Using a subset of mice in which 110 neurons were recorded simultaneously (n = 3), we sub-sampled groups of neurons from the entire population (10 repetitions per animal per condition), and computed principal components based on the smaller neural population. In this restricted dataset, the neural encoding of both joint angles and movement vector pairs improves with increasing numbers of neurons. While joint angle encoding remains significantly better than movement vector encoding until 110 neurons are included in the population (the maximum number tested; Figure 3D), the difference decreases as the number of sub-sampled neurons grows. Thus, a larger population of neurons is required for somatosensory cortex to abstract from neural encoding of joint angles into a movement vector. In conclusion, population-level analysis shows that movement vectors are encoded by large populations in mouse sensorimotor cortex, supporting prior inferences from analysis of single neurons [1].

3.3 Orthogonality between ipsilateral and contralateral limb representations

The structure of neural representations within motor cortex extends beyond low dimensionality of neural responses. For example, neural representations of both ipsilateral and contralateral limbs in motor cortex co-exist within a single cortical hemisphere yet occupy distinct and orthogonal subspaces [37]. To examine if this same organization exists for somatosensory information from the ipsilateral and contralateral limbs, we used PCA to define a low-dimensional space for neural responses of the anesthetized animals to passive limb movements. We optimized the principal components for neural responses to contralateral or ipsilateral limbs by conducting PCA on trials corresponding to passive deflections of only contralateral or ipsilateral limbs. The results show that the PCs that best capture variance in neural responses to the contralateral limb movements ("Contra") do a poor job of explaining neural activity related to movement of the ipsilateral limb, and vice versa (Figure 4A, B). In these specialized sub-spaces, the angle between neural trajectories for ipsilateral and contralateral limbs is close to 90 degrees. (Figure 4C). Therefore, the neural representation of contralateral and ipsilateral limbs within sensorimotor cortex is orthogonal to each other, analogous to encoding of motor commands.

3.4 Conserved representations across animals

A final question is to determine whether the low-dimensional representation of somatosensation is conserved across animals. For example, within the motor cortex, neural dynamics underlying motor control are well conserved within an animal across time (robust to changes in the recorded neural population), across animals performing the same task, and even across species performing similar behaviors [48, 49]. To address this question, we used canonical correlations analysis (CCA) to map the trial-average neural trajectories from pairs of animals into the same subspace [29, 48, 49]. In anesthetized animals we analyzed the degree of overlap between neural representations of distinct limbs; in awake animals, we analyzed the degree of overlap between movements of a singe limb in different directions. Directly comparing neural encoding of separate limb movements across the anesthetized animals or different directions of a limb across the awake animals is not possible on a trial-to-trial basis due to the variability in limb movements. To compare across animals, we therefore averaged neural

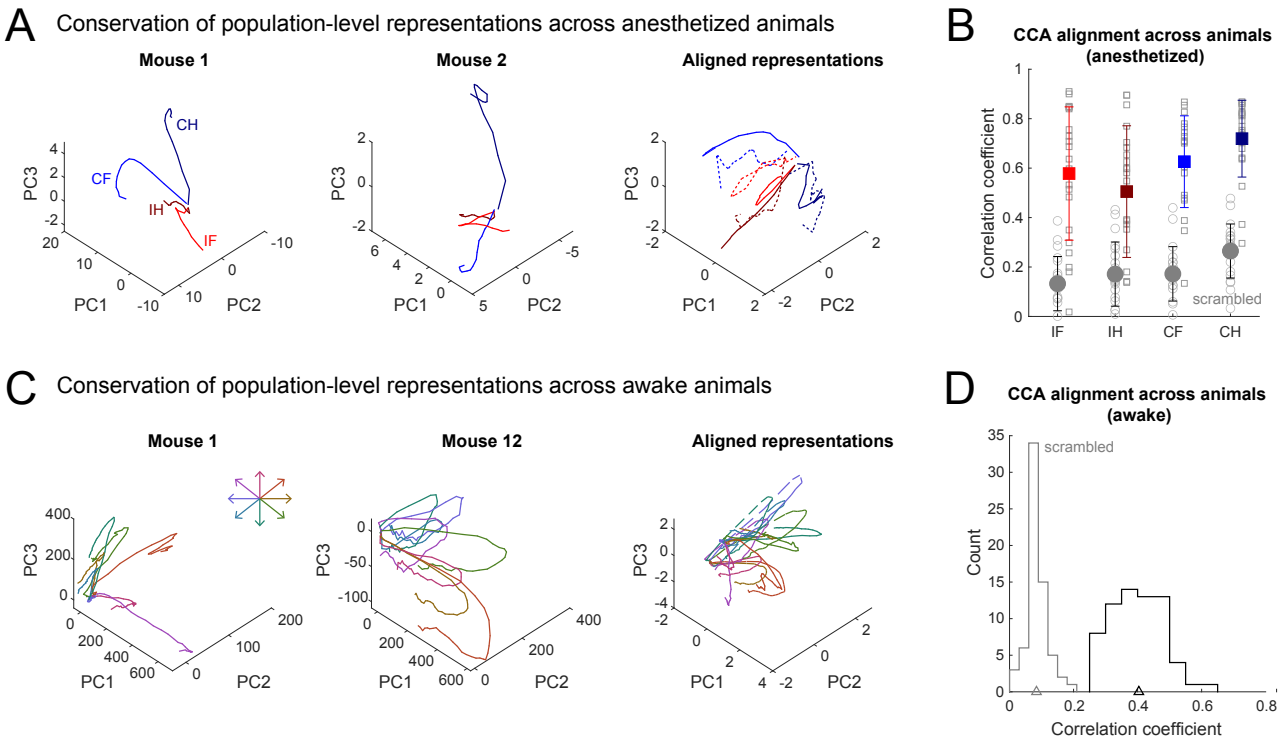

Figure 5: Conservation of the structure of neural representations of limb somatosensation across animals. **A.** Left and center: Example neural trajectories associated with single-limb deflections during anesthesia in two sample mice. Right: aligned representations following CCA. CH: contralateral hindlimb, CF: contralateral forelimb, IH: ipsilateral hindlimb, IF: ipsilateral forelimb. **B.** Pairwise correlation between aligned neural trajectories for single limb movements across mice (e.g., CH_{mouse1} with CH_{mouse2}). Colors as in (A). Scrambled (gray) refers to alignment of randomly-permuted matrices. **C.** Left and center: Example neural trajectories associated with awake center-out forelimb deflections in two sample mice. Right: aligned representations following CCA. The inset in the first panel shows a color code for each movement direction. **D.** Pairwise correlation between aligned neural trajectories for movement vectors across mice (black line). Scrambled (gray) refers to alignment of randomly-permuted matrices.

trajectories across all trials associated with deflection of a single limb for the anesthetized animals or a direction for the awake animals to obtain separate representative trajectories for different limbs or directions within the low dimensional space (one trajectory per limb in Figure 5A; one trajectory per direction in Figure 5C). CCA was then performed on the matched neural response matrices across pairs of animals. Given two matrices (here, the low-dimensional subspaces associated with somatosensation from two animals), CCA identifies a set of linear transformations that maximally correlate those matrices. Then, the normalized dot product between matched trajectories within this new subspace was used to quantify the degree of matching between animal pairs.

We found that the low-dimensional representations of somatosensation are well conserved across both awake and anesthetized animals (Figure 5). As a control, we also performed CCA between true and scrambled datasets; the latter manipulation breaks both the correlations between neurons and the temporal relationship of the dataset but maintains average activity levels. The alignment with scrambled datasets was significantly lower than the true datasets for all limbs (Figure 5B,D), which shows that CCA cannot align arbitrary pairs of matrices. However, note that increasing the number of dimensions used for alignment can improve alignment, even for arbitrary matrices (Figure S1).

4 Discussion

The purpose of this manuscript was to investigate the structure of neural activity within mouse sensorimotor cortex as it relates to somatosensory inputs from the limbs. Our major idea was to "summarize" activity within a large population of neurons by using principal component analysis – a standard form of dimensionality reduction that identifies correlated activity across independent variables (here, across neurons). Using these low-dimensional representations, we were able to establish that the structure of neural activity in mouse sensorimotor cortex mirrors the observed low-dimensional encoding of motor commands and is well preserved across animals (Figures 2,5), including maintaining orthogonal representations of ipsilateral and contralateral limbs (Figure 4). This population-level approach additionally yielded insight into the way that neural populations encode variables that differ from single neuron encoding. We found that an extrinsic representation of limb movements (a movement vector) can emerge from a population of neurons, while activity of individual neurons best correlates with intrinsic representations, such as changes in joint angles (Figure 3). Together, our results illustrate how the structure of neural representations in sensorimotor may facilitate sensorimotor integration across the brain.

4.1 Somatosensation includes both touch and proprioception

Somatosensation encompasses two classes of sensory inputs, touch and proprioception, which activate neural responses in overlapping brain regions [1]. Within the somatosensory cortex, touch and proprioception recruit distinct populations of neurons such that blocking tactile inputs does not significantly alter the responses of proprioceptive-encoding neurons to passive limb movements [1]. Therefore, tactile sensations induced during the course of the experiments described here (primarily pressure upon the paw(s) from the experimenter or induced by the animal's grasp of the robotic manipulandum) would be expected to activate separate subpopulations of recorded neurons that could potentially increase the total dimensionality of neural activity. While touch has the capacity to be a high-dimensional signal in the sense that higher PCs can be used to accurately identify the texture presented to an animal [50], we found in this current study that neural activity in responses to somatosensory inputs were low-dimensional. Notably, even when touch is considered high-dimensional (as in primate neural encoding of texture), the first two PCs explain approximately 80% of the variability in neural responses to textures [50], suggesting that somatosensation is generally a low-dimensional sensory signal. That is, neural activity patterns across neurons are correlated and can be well summarized by a relatively small number of PCs relative to the size of the simultaneously recorded neural population. However, there is some evidence that there are distinct neural mechanisms for encoding texture in the mouse and in the primate. In the study referenced above [50], the first PC was most strongly correlated with the roughness of a texture, which dominated the time-varying changes in neural activity patterns. In contrast, neural activity in mouse somatosensory cortex isn't time-locked to vibration frequency (which could encode roughness), but instead neurons are tuned to specific input frequencies [51]. This encoding mechanism could increase the dimensionality of the touch signal in mouse cortex, but the datasets analyzed in this current manuscript are not designed to evaluate this possibility.

4.2 The intrinsic dimensionality of somatosensation

Must the neural encoding of somatosensation in mouse sensorimotor areas be low-dimensional? We discussed some implications for the dimensionality of touch in the previous section, so we focus here on proprioception. The sense of proprioception is based on sensors embedded in the tendons, muscles, and joints that are active both during static limb configurations and during dynamic changes in posture [6]. Receptor activity conveys redundant information about twenty-two muscles in the mouse forelimb and forty muscles in the hindlimb [52, 53], which form a smaller number of functional groups that

enact coordinated activity across multiple muscles. For example, in the mouse hindlimb, muscles coordinate to rotate, flex, or extend the knee, hip, and ankle [53]. At an even more abstract level, limb posture and movement can be represented simply as a set of joint angles (of the hip, knee, and ankle), changes in which are highly correlated across limb movements [54]. Movement can also be represented as a vector that, unlike joint angles, is independent of the starting and end points of the reach (e.g., distance and direction). Therefore, there are relatively few independent variables to encode by the hundreds of thousands of neurons in sensorimotor cortical areas [43]. In consequence, a reasonable hypothesis regarding the dimensionality of proprioceptive information within the cortex is that it would be low-dimensional. While we find this to be the case, neural anatomy suggests that the dimensionality of sensory information *could* increase along the cortical hierarchy, as the number of neurons in the cortex is roughly an order of magnitude larger than in the thalamus [43, 44]. This significant anatomical expansion could have mediated an expansion of the dimensionality of the representation of proprioceptive inputs within sensorimotor cortex [45]. Therefore, the dimensionality of somatosensory information in the cortex is not obvious a priori.

4.3 Robustness of results across datasets

We used three complementary datasets (anesthetized passive multi-limb, awake passive forelimb, and awake active multi-limb) to show that somatosensory information from the limbs occupies a low-dimensional subspace within the neural population response, regardless of the behavioral state of the animal. The anesthetized data is valuable because it contains the responses of neurons within mouse sensorimotor cortex to passive deflection of each of the four limbs. These deflections were performed manually, which resulted in high trial-to-trial variability in limb trajectories within an acute range of angles (Figure S2). High variability in limb trajectories is critical to estimating the true dimensionality of proprioceptive information, as dimensionality is reduced during highly stereotyped movements [55].

Analysis of the awake datasets were essential to validate the hypotheses generated from the anesthetized data, including verifying that the measured dimensionality does not come simply from changes in network structure during anesthesia [56, 57]. In the awake passive forelimb experiments conducted by another lab and shared with the neuroscience community [1, 58], mice held a robotic manipulandum during passive movements in both center-out and out-center directions (Figure 1B). Unlike passive movements under anesthesia, here, the mouse's forelimb was moved over a wide range of angles (in eight directions from 0 to 360 degrees). However, given the robotic control of the movements, limb movements in any particular direction were highly stereotyped, which might artificially depress the dimensionality of neural responses [55]. The second awake dataset, collected from awake, head-fixed mice that were free to run or rest on a styrofoam ball [59, 60], included recordings made from sensorimotor cortex during active movements. Therefore, the behavior of the animals was more variable than in either of the other two datasets, but the neural activity patterns also likely include input from motor-related areas rather than a pure proprioceptive signal [61]. The variability in experimental conditions across these datasets ensures the robustness of our conclusions, as we see a similar relationship between the fraction of significant PCs to the cumulative proportion of variance explained across datasets (Figure 2).

4.4 Movement vectors vs. joint angles

We found that neural activity patterns in principal component space represented movement vectors as well as joint angles when the principal components were calculated based on the activity of a large population of neurons (at least 75 neurons; Figure 3). Why should proprioceptive inputs be represented in the form of a movement vector rather than more concretely as changes in joint angles? One possibility, suggested by computational modeling, is that in many sensorimotor tasks, *"what"* needs

to be done is invariant to *"where"* it is being done in space [62]. This type of "what" representation has been observed in higher brain areas, including the parietal and premotor cortices, which tend to encode movement intention rather than limb kinematics [63, 64, 65]. Furthermore, premotor cortex is known to convey movement intention (efference copy) to somatosensory cortex [66]. Therefore sensorimotor cortex may abstract changes of joint angles into vectorial representations of movement in order to efficiently communicate with higher brain areas. It is important to note that "movement vector" representations only arise in principal component space after neural activity in the population has been projected onto the identified principal components via matrix multiplication; it is not evident when simply considering the unmanipulated neural activity of the population (Figure 3). Therefore, the extraction of a movement vector may not happen locally; instead, it may be implemented via projections into higher brain areas.

Human and animal perception seems to better align with extrinsic vs instrinsic variables [1, 67, 68]. For example, mice are more likely classify passive limb movements according to the direction of movement relative to the body (towards vs. away) rather than by the changes in joint angles elicited by that movement [1], and humans are more precise at aligning a cursor with their hand position than at rotating a line to match a joint angle [68]. Furthermore, electrical microstimulation of the human parietal cortex elicits proprioceptive sensations that describe the direction of movement (upwards, forward, etc. [67]), which emphasizes that our conscious experience of movement is its direction – an extrinsic variable.

4.5 Implications for clinical neural prostheses

Our population-level analysis of neural activity in sensorimotor cortex of mice has shown that the encoding of somatosensation mirrors that found in other cortical areas involved in sensorimotor processing, and that this similarity could facilitate the integration of information across brain areas. This basic scientific result has important implications for neural prostheses, as somatosensory cortex is seen as a key anatomical target for neuromodulation to provide artificial sensation in bidirectional brain-machine interfaces [69, 70, 71, 72, 73, 74]. Understanding how somatosensation, including proprioception, is encoded in sensorimotor cortex will help us design optimal artificial sensory signals that will integrate with natural sensation and ultimately improve the performance and embodiment of neural prostheses [75, 76, 77, 78].

5 Methods

5.1 Mice

All procedures were approved by the Institutional Animal Care and Use Committee at Purdue University. Eight CaMKII-tTA (JAX stock #007004) x TRE-GCaMP6s (JAX stock #024742) mice aged 3-6 months were used for 2-photon calcium imaging. Mice were housed in groups of no more than five per cage in a temperature and humidity-controlled room on a 12-hour light/dark cycle with *ad libitum* access to food and water.

5.2 Surgical Procedures

For all surgical procedures, mice were anesthetized with isoflurane at 3% for induction and maintained between 1.5-2.5% to areflexia. All mice were first surgically implanted with a custom titanium headplate (8 mm circular inner diameter) placed over the right cortical hemisphere and secured with dental cement. Allowing at least three days for recovery, a 5 mm craniectomy was then made over the primary somatosensory and primary motor cortical areas (stereotaxic anatomical coordinates determined from Paxinos & Franklin). A 5 mm round glass window was placed over the brain and secured

with a cyanoacrylate mixture. Mice were then given at least three days to recover from surgery before undergoing imaging.

5.3 Proprioception Experiment

Mice were first anesthetized with isoflurane at 3% for induction and maintained at 0.9-1.1% to preserve neural activity during recordings. A heating pad maintained at 37°C (World Precision Instruments) was placed under the mice for the duration of anesthesia. Mice were carefully examined throughout the duration of the experiment for respiratory pattern and areflexia to ensure a consistent level of anesthesia. The mouse's headplate was secured to a custom headplate holder to fix the head for two-photon imaging (Neurolabware microscope, Scanbox software). Limb movement during the experiment was video recorded at 30 fps (The Imaging Source).

Two-photon imaging in 1x magnification (approx. 1.9 x 1.2 mm FOV) was performed to determine the representation of limb movement over the sensorimotor cortex. The imaging windows were positioned in various locations over sensorimotor cortex (Figure S3) to obtain neural recordings across the entire region. Passive limb movement was performed by manually brushing the entire limb, starting at an area of the limb close to the trunk and moving towards the paw. This was done to each limb five times for three cycles, with a total of 15 passive movements for each limb. The order of limb movement was randomized for each mouse, and ample time ($\sim$10 seconds) was given between each movement to allow the fluorescent signal to return to baseline levels before the next movement.

Two-photon images were processed using Suite2p [79], an image processing pipeline that performs image registration, cell detection, and signal extraction from detected cells. Extracted fluorescence traces were processed and neuropil signals were removed by subtracting neuropil signals multiplied by 0.7 and standardized (z-scored).

5.4 Principal component analysis (PCA) and dimensionality analysis

PCA was performed using *sklearn.decomposition.PCA* in Python for Figure 2 and Figure 4 and MATLAB for Figure 1 and Figure 5. Three types of data were used for the analysis from (1) the anesthetized mice, (2) the awake mice, and (3) the running mice [41]. More details about the running mice data can be found from the source [41]. PCA was used in this manuscript as a method of dimensionality reduction. For the awake freely running mice (with spontaneous, self-generated movements), neural responses were not separated into individual trials and instead PCA was conducted on the z-scored matrix of *[total recorded timepoints, neurons]*. For the anesthetized and awake passive movement mice, multiple trials were conducted within each recording session for each animal. Prior to PCA, single-trial responses were extracted from the total recorded session. The response of a single neuron to passive movement on a single trial was taken relative to the baseline fluorescence (the value of the neural activity just prior to movement onset). For anesthetized mice, trial onset and offset was defined as the neural imaging frame on which movement began and ended, which was manually identified from the concurrent 30 fps video recordings during the experiments. For awake mice, limb movements were trial onset and offset were defined as in [1] and computed using the provided open-source code [58].

The total neural response of a population of neurons to a set of trials was found to be a tensor of size [the number of trials, the number of time points per trial, the number of neurons]. As described above, in the case of the anesthetized data, the number of timepoints per trial could vary. We used PCA to compute the dimensionality of the neural responses under two conditions. First, we used the average across time points within each trial ([trials, neurons]; *ANES-AVG* and *AWAKE-AVG* in Figure 2), which yielded a single value per trial. Second, used the responses during the entire trial, concatenating the data across trials ([trials$\times$time points, neurons]; *ANES-CONCAT* and *AWAKE-CONCAT* in Figure 2). The first strategy results in projections of shape [trials, total PCA components]

and the second results in projections of shape [trials×time points, total PCA components]. The total number of PCA components that can be found is constrained by the smallest dimension in these matrices, i.e. *min(trials, neurons)* or *min(trials×time points, neurons)*.

To determine the significant PCs among the total components, we compared eigenvalues from the original data and 100 randomly permuted matrix [46]. When the number of random cases which has a higher eigenvalue than the original data normalized by the number of permuted matrix (100 in this case) was higher than 0.05, that component was determined as significant. Since the number of significant PCs can be affected by the total number of PCs, we also normalized it by the number of total components (Figure 2B). The shape of the data, the shape of the projections, the significant components, and the variance explained of the significant components are specified in Tables S1-3.

5.5 Decoding somatosensation from cumulative PCA components

Cumulative PCs were used to decode somatosensation, i.e. which limb was targeted for a trial for anesthetized mice and which direction (angle) among eight directions was provided for the passive movement for a trial for awake mice. Linear discriminant analysis was used as a decoder. For training and testing, leave-one-out cross-validation was used in which the average score of the combinations of one trial as test data and the other trials as train data was reported as a result. In addition to the accuracy, accuracy±1 was reported for awake animals. Accuracy±1 was calculated as the sum of the number of trials within the true direction and two adjacent directions divided by the total number of trials. For example, if the true direction label was 2 among the whole labels from 0 to 7, it was counted as being correct if the prediction was one of 1, 2, or 3. It was designed considering that the classes of directions are continuous in a circular way, therefore to see if the prediction was close to the correct class.

5.6 Neural encoding of joint angles vs. movement vectors

This analysis was conducted on neural data from [1], using their provided MATLAB code to extract neural responses to single trials. *Neural space:* A three-dimensional neural response tensor was then found for each mouse [trials, timepoints per trial, neurons]. Trials included successfully completed center-out and out-center movements (see Figure 1B). Finally, a trial-averaged neural response trajectory was found for each movement in each of the outwards and inward directions. *PC space:* The neural response tensor was converted into a two-dimensional matrix of size [trials× timepoints per trial, neurons]. The PCs of this matrix were then found using the MATLAB function *pca*, and the original neural response tensor was projected onto the first five PCs (approximately the average number of significant components found for individual mice in this dataset). This formed the PC space. Finally, a trial-averaged neural response trajectory was found for each movement in each of the outwards and inward directions.

To determine whether the neural population activity best encoded joint angles or movement vectors, we computing the correlation between pairs of neural trajectories in both *neural space* and *PC space*. Correlation was calculated as a dot product between trial-averaged neural response vectors ($\vec{r_i}$), divided by the length (norm) of each vector: $\rho_{1,2} = \vec{r_1}\vec{r_2}/(|\vec{r_1}||\vec{r_2}|)$. Given the asymmetry of neural responses across movement vectors [1], correlations were only calculated for movements towards the body (center-out movements 4 - 8, corresponding to movements in between 135° and 315°. To measure similarity between movement vector pairs, we calculated the correlations between center-out movements [4:8] and out-center movements [1,5:8]. To measure similarity between joint angle pairs, we used the minimum of the correlations between the neural response to center-out movement i and the neural response to center-out movement $i-1$ and $i+1$, where $i \in [4:8]$.

To examine the relationship between neural encoding and neural population size, we identified a

subset of mice (n = 3) in which at least 110 neurons were imaged simultaneously. We repeated the process described above using subsample of the entire neural population (sampling with replacement a set of [10, 25, 50, 75, 100, and 110] neurons from each mouse, 10 repetitions of each size).

5.7 Orthogonality between the projections of ipsilateral and contralateral limb representations

Two different PC spaces were obtained using the neural responses of the anesthetized animals for contralateral limbs and ipsilateral limbs, separately ("Contra" and "Ipsi" in Figure 4). The variances explained of the contralateral responses projected onto the "Contra" and the "Ipsi" were both normalized by the sum of the variance explained of the contralateral responses projected onto the "Contra" because it is the available maximum. Similarly, the variances explained of the ipsilateral responses projected onto the "Contra" and the "Ipsi" were both normalized by the sum of the variance explained of the ipsilateral responses projected onto the "Ipsi". To calculate the angle between the ipsilateral and contralateral projections, resampled and trial-averaged neural responses were used for PCA. Dot product was performed on the flattened vectors from the trial-averaged responses projections onto "Contra", and "Ipsi", which was converted into the angle in degree.

5.8 Conserved representations across animals

To test for the similarity of neural representations of limbs movements across animals, we used CCA to align the average neural trajectories associated with movement of each limb (anesthetized mice) or associated with each movement direction (center-out passive movements in awake mice). For the anesthetized dataset, trials were of variable length, and the entire trial was used to compute the PCs of the neural responses. However, to compute the average neural trajectory associated with each limb movement, neural activity in each trial was resampled to acquire the response over the first two seconds (15 samples at 7.8 Hz sampling rate) following movement onset [trials, 15 timepoints, neurons]. A duration of 15 samples was chosen as it was the mode of the unaltered trial durations. This neural response matrix was permuted to yield a matrix of size [trials$\times$15, neurons] and was then projected onto the first three PCs (within the lower end of range of significant components of this type of dataset for the animals). After permuting the matrix once more into a tensor [trials, 15 timepoints, 3 PCs], the trials associated with movement of each limb were averaged to generate a matrix of average responses to passive deflection of each limb [15 timepoints, 3 PCs]. This process was repeated for each mouse, yielding eight neural response matrices. Then, we used the MATLAB function *canoncorr* to map neural response matrices from pairs of mice into a common reference frame. Once the data was in the same reference frame, we calculated the correlation between the neural trajectories associated with each limb from each mouse (using the same equation described above). As a control, the original data matrix was shuffled [trials$times$timepoints, neurons], over both the rows and columns, and the true data from one mouse in each pair was mapped to the shuffled representation. This calculation sets a baseline level for how well CCA can match two matrices when one of them is meaningless (random). Note, however, that the correlations depend on the number of PCs that are chosen. As this number grows, arbitrary matrices can be flexibly mapped to one another (Figure S1).

The same analysis was repeated for the awake dataset, but as the trials were of equal lengths, there was no need to resample neural data.

6 Acknowledgments

This work was supported by the National Science Foundation as part of the HDR Institute: Accelerated AI Algorithms for Data-Driven Discovery (award #2117997). We thank Elizabeth Frazier for providing

valuable feedback on the analyses in this manuscript.

References

[1] Ignacio Alonso et al. "Peripersonal encoding of forelimb proprioception in the mouse somatosensory cortex". In: *Nature Communications* 14 (2023), p. 1866.

[2] Seungbin Park, Megan Lipton, and Maria C. Dadarlat. "Decoding multi-limb movements from low temporal resolution calcium imaging using deep learning". In: *bioRxiv* (2023). eprint: `https://www.biorxiv.org/content/early/2023/12/03/2023.11.30.569459.full.pdf`.

[3] John C. Tuthill and Eiman Azim. "Proprioception". In: *Current Biology* 28.5 (2018), R194–R203.

[4] Roland S Johansson and J Randall Flanagan. "Coding and use of tactile signals from the fingertips in object manipulation tasks." In: *Nature reviews. Neuroscience* 10.5 (2009), pp. 345–59.

[5] Gregg A. Tabot et al. "Restoring tactile and proprioceptive sensation through a brain interface". en. In: *Neurobiology of Disease* 83 (Nov. 2015), pp. 191–198.

[6] Benoit P. Delhaye, Katie H. Long, and Sliman J. Bensmaia. "Neural basis of touch and proprioception". In: *Compr Physiol.* 8.4 (2018), pp. 1575–1602.

[7] Gregg A. Tabot et al. "Restoring the sense of touch with a prosthetic hand through a brain interface". en. In: *Proceedings of the National Academy of Sciences* 110.45 (Nov. 2013), pp. 18279–18284.

[8] R L Sainburg, H Poizner, and C Ghez. "Loss of proprioception produces deficits in interjoint coordination." In: *Journal of neurophysiology* 70.5 (1993), pp. 2136–2147.

[9] R L Sainburg et al. "Control of limb dynamics in normal subjects and patients without proprioception." In: *Journal of neurophysiology* 73.2 (Feb. 1995), pp. 820–835.

[10] Georgina M. Jackson et al. "The coordination of bimanual prehension movements in a centrally deafferented patient". In: *Brain* 123.2 (2000), pp. 380–393.

[11] Esther Kuehn et al. "On the bimanual integration of proprioceptive information". In: *Experimental Brain Research* 233.4 (2015), pp. 1273–1288.

[12] Jacob E. Schaffer, Fabrice R. Sarlegna, and Robert L. Sainburg. "A rare case of deafferentation reveals an essential role of proprioception in bilateral coordination". In: *Neuropsychologia* 160 (2021), p. 107969.

[13] A. J. Suminski et al. "Incorporating Feedback from Multiple Sensory Modalities Enhances Brain-Machine Interface Control". In: *Journal of Neuroscience* 30.50 (Dec. 2010), pp. 16777–16787.

[14] Raeed H. Chowdhury, Joshua I. Glaser, and Lee E. Miller. "Area 2 of primary somatosensory cortex encodes kinematics of the whole arm". In: *eLife* 9 (2020), pp. 1–31.

[15] M J Prud'homme and J F Kalaska. "Proprioceptive activity in primate primary somatosensory cortex during active arm reaching movements." In: *Journal of neurophysiology* 72.5 (1994), pp. 2280–301.

[16] Brian M London and Lee E Miller. "Responses of somatosensory area 2 neurons to actively and passively generated limb movements." In: *Journal of neurophysiology* 109.6 (Dec. 2013), pp. 1505–13.

[17] Aneesha K. Suresh et al. "Neural population dynamics in motor cortex are different for reach and grasp". In: *eLife* 9 (2020), pp. 1–16.

[18] Douglas J. Weber et al. "Limb-state information encoded by peripheral and central somatosensory neurons: Implications for an afferent interface". In: *IEEE Transactions on Neural Systems and Rehabilitation Engineering* 19.5 (Aug. 2011), pp. 501–513. eprint: NIHMS150003.

[19] Oleg V. Favorov et al. "Activity of somatosensory-responsive neurons in high subdivisions of SI cortex during locomotion". In: *Journal of Neuroscience* 35.20 (2015), pp. 7763–7776.

[20] Raeed H. Chowdhury, Matthew C. Tresch, and Lee E. Miller. "Musculoskeletal geometry accounts for apparent extrinsic representation of paw position in dorsal spinocerebellar tract". In: *Journal of Neurophysiology* 118.1 (2017), pp. 234–242.

[21] James M. Goodman et al. "Postural Representations of the Hand in the Primate Sensorimotor Cortex". In: *Neuron* 104.5 (2019), 1000–1009.e7.

[22] Alice Lucas et al. "Neural networks for modeling neural spiking in S1 cortex". In: *Frontiers in Systems Neuroscience* 13 (2019).

[23] Daniel Wolpert, Z Ghahramani, and MI Jordan. "An internal model for sensorimotor integration". In: *Science* 269.5232 (Sept. 1995), pp. 14–16.

[24] Zoubin Ghahramani, Daniel M. Wolpert, and Michael I Jordan. "Computational models of sensorimotor integration". In: *Advances in Psychology* 119.C (1997), pp. 117–147.

[25] Seth W. Egger et al. "Internal models of sensorimotor integration regulate cortical dynamics". In: *Nature Neuroscience* 22.11 (2019), pp. 1871–1882.

[26] John P Cunningham and Byron M Yu. "Dimensionality reduction for large-scale neural recordings". en. In: *Nature Neuroscience* 17.11 (Nov. 2014), pp. 1500–1509.

[27] Carsen Stringer and Marius Pachitariu. "Analysis methods for large-scale neuronal recordings". In: *Science* 386 (2024), eadp7429.

[28] John K. Chapin and Miguel A.L. Nicolelis. "Principal component analysis of neuronal ensemble activity reveals multidimensional somatosensory representations". In: *Journal of Neuroscience Methods* 94.1 (1999), pp. 121–140.

[29] John P Cunningham and Zoubin Ghahramani. "Linear Dimensionality Reduction: Survey, Insights, and Generalizations". In: *Journal of Machine Learning Research* 16 (2015), pp. 2859–2900. eprint: 1406.0873.

[30] Wujie Zhang et al. "Coupling between One-Dimensional Networks Reconciles Conflicting Dynamics in LIP and Reveals Its Recurrent Circuitry". In: *Neuron* 93.1 (2017), pp. 221–234.

[31] Luciano Dyballa et al. "Population encoding of stimulus features along the visual hierarchy". In: *Proceedings of the National Academy of Sciences of the United States of America* 121.4 (2024), pp. 1–11.

[32] Noel Federman et al. "Acquisition of non-olfactory encoding improves odour discrimination in olfactory cortex". In: *Nature Communications* 15.1 (2024), pp. 1–19.

[33] Mark M Churchland et al. "Neural Population Dynamics During Reaching". In: *Nature* 487.7405 (June 2012), pp. 1–20. eprint: NIHMS150003.

[34] Hansem Sohn et al. "A Network Perspective on Sensorimotor Learning". In: *Trends in Neurosciences* 44.3 (2020), pp. 170–181.

[35] K V Shenoy, M Sahani, and M M Churchland. "Cortical control of arm movements: a dynamical systems perspective". In: *Annual Review of Neuroscience* 36.May (May 2013), pp. 337–359.

[36] Mark M. Churchland and Krishna V. Shenoy. "Preparatory activity and the expansive nullspace". In: *Nature Reviews Neuroscience* 25 (4 2024), pp. 213–236.

[37] Katherine Cora Ames and Mark M. Churchland. "Motor cortex signals for each arm are mixed across hemispheres and neurons yet partitioned within the population response". In: *eLife* 8 (2019), pp. 1–36.

[38] Ethan A. Heming et al. "Independent representations of ipsilateral and contralateral limbs in primary motor cortex". In: *eLife* 8.2002 (2019), pp. 1–26.

[39] John E. Downey et al. "The motor cortex has independent representations for ipsilateral and contralateral arm movements but correlated representations for grasping". In: *Cerebral Cortex* 30.10 (2020), pp. 5400–5409.

[40] Aurélie Pala and Garrett B. Stanley. "Ipsilateral Stimulus Encoding in Primary and Secondary Somatosensory Cortex of Awake Mice". In: *Journal of Neuroscience* 42.13 (2022), pp. 2701–2715.

[41] Seungbin Park, Megan Lipton, and Maria C Dadarlat. "Decoding multi-limb movements from two-photon calcium imaging of neuronal activity using deep learning". In: *J. Neural Eng.* 21.6 (Dec. 2024), p. 066006.

[42] Seungbin Park, Megan Lipton, and Maria Dadarlat. *Decoding multi-limb movements from two-photon calcium imaging of neuronal activity using deep learning.* Mendeley Data, V1, doi:10.17632/rk2xywhx7w Aug. 2024.

[43] Marian Evangelio, María García-Amado, and Francisco Clascá. "Thalamocortical projection neuron and interneuron numbers in the visual thalamic nuclei of the adult C57BL/6 mouse". In: *Frontiers in Neuroanatomy* 12.April (2018), pp. 1–12.

[44] Suzana Herculano-Houzel, Charles Watson, and George Paxinos. "Distribution of neurons in functional areas of the mouse cerebral cortex reveals quantitatively different cortical zones". In: *Frontiers in Neuroanatomy* 7.OCT (2013), pp. 1–14.

[45] Srdjan Ostojic and Stefano Fusi. "Computational role of structure in neural activity and connectivity". In: *Trends in Cognitive Sciences* 28.7 (2024), pp. 677–690.

[46] Scott B. Franklin et al. "Parallel Analysis: a method for determining significant principal components". en. In: *Journal of Vegetation Science* 6.1 (Feb. 1995), pp. 99–106.

[47] Peiran Gao and Surya Ganguli. "On simplicity and complexity in the brave new world of large-scale neuroscience". en. In: *Current Opinion in Neurobiology* 32 (June 2015), pp. 148–155.

[48] Juan A. Gallego et al. "Long-term stability of cortical population dynamics underlying consistent behavior". In: *Nature Neuroscience* 23.2 (2020), pp. 260–270.

[49] Mostafa Safaie et al. "Preserved neural dynamics across animals performing similar behaviour". In: *Nature* 623.7988 (2023), pp. 765–771.

[50] Justin D. Lieber and Sliman J. Bensmaia. "High-dimensional representation of texture in somatosensory cortex of primates". In: *Proceedings of the National Academy of Sciences of the United States of America* 116.8 (2019), pp. 3268–3277.

[51] Mario Prsa et al. "Feature-selective encoding of substrate vibrations in the forelimb somatosensory cortex". In: *Nature* 567.7748 (2019), pp. 384–388.

[52] Margie A. Mathewson et al. "Anatomical, architectural, and biochemical diversity of the murine forelimb muscles". In: *Journal of Anatomy* 221.5 (2012), pp. 443–451.

[53] James P. Charles et al. "Musculoskeletal geometry, muscle architecture and functional specialisations of the mouse hindlimb". In: *PLoS ONE* 11.4 (2016).

[54] Max Grogan et al. "Predicting proprioceptive cortical anatomy and neural coding with topographic autoencoders". In: *PLoS Computational Biology* 20.12 (2024), e1012614.

[55] Zengcai V. Guo et al. “Flow of cortical activity underlying a tactile decision in mice”. In: *Neuron* 81 (1 2014), pp. 179–194.

[56] Bilal Haider, Michael Häusser, and Matteo Carandini. “Inhibition dominates sensory responses in the awake cortex.” In: *Nature* 493.7430 (Jan. 2013), pp. 97–100.

[57] Kristin K. Sellers et al. “Awake vs. anesthetized: Layer-specific sensory processing in visual cortex and functional connectivity between cortical areas”. In: *Journal of Neurophysiology* 113.10 (2015), pp. 3798–3815.

[58] Mario Prsa. *CodeData AlonsoScheer et al NatComm 2023*. Feb. 2023.

[59] Seungbin Park, Megan Lipton, and Maria Dadarlat. *DATASET Decoding multi-limb movements from two-photon calcium imaging of neuronal activity using deep learning*. Version V1. 2024.

[60] Seungbin Park, Megan Lipton, and Maria C. Dadarlat. “Decoding multi-limb movements from two-photon calcium imaging of neuronal activity using deep learning”. In: *Journal of neural engineering* 21.6 (2024).

[61] Tianyi Mao et al. “Long-Range Neuronal Circuits Underlying the Interaction between Sensory and Motor Cortex”. In: *Neuron* 72.1 (2011), pp. 111–123.

[62] Kai J. Sandbrink et al. “Contrasting action and posture coding with hierarchical deep neural network models of proprioception”. In: *eLife* 12 (2023), pp. 1–29.

[63] Richard A. Andersen and He Cui. “Intention, Action Planning, and Decision Making in Parietal-Frontal Circuits”. In: *Neuron* 63.5 (Sept. 2009), pp. 568–583.

[64] Janina Klautke et al. “Dynamic spatial coding in parietal cortex mediates tactile-motor transformation”. In: *Nature Communications* 14.1 (2023).

[65] L Shen and G E Alexander. “Preferential representation of instructed target location versus limb trajectory in dorsal premotor area.” In: *Journal of neurophysiology* 77.3 (1997), pp. 1195–1212.

[66] Mark Schram Christensen et al. “Premotor cortex modulates somatosensory cortex during voluntary movements without proprioceptive feedback”. In: *Nature Neuroscience* 10.4 (2007), pp. 417–419.

[67] Michelle Armenta Salas et al. “Proprioceptive and cutaneous sensations in humans elicited by intracortical microstimulation”. In: *eLife* 7 (2018), pp. 1–11.

[68] Christina T. Fuentes and Amy J. Bastian. “Where is your arm? Variations in proprioception across space and tasks”. In: *Journal of Neurophysiology* 103.1 (2010), pp. 164–171.

[69] S. N. Flesher et al. “Intracortical microstimulation of human somatosensory cortex”. In: *Science Translational Medicine* 8.361 (2016), 361ra141–361ra141.

[70] Christopher L. Hughes et al. “Perception of microstimulation frequency in human somatosensory cortex”. In: *eLife* 10 (2021), pp. 1–19.

[71] Gregg a Tabot et al. “Restoring the sense of touch with a prosthetic hand through a brain interface.” In: *Proc. Natl. Acad. Sci. U. S. A.* 110.45 (2013), pp. 18279–84.

[72] Thierri Callier et al. “The frequency of cortical microstimulation shapes artificial touch”. In: *Proceedings of the National Academy of Sciences of the United States of America* 117.2 (Jan. 2020), pp. 1191–1200.

[73] Tucker Tomlinson and Lee E Miller. “Toward a Proprioceptive Neural Interface That Mimics Natural Cortical Activity Tucker”. In: *Adv Exp Med Biol.* 957 (2016), pp. 367–388.

[74] Emily Graczyk et al. "Clinical Applications and Future Translation of Somatosensory Neuroprostheses". In: *The Journal of neuroscience : the official journal of the Society for Neuroscience* 44.40 (2024).

[75] Karthik Kumaravelu et al. "A comprehensive model-based framework for optimal design of biomimetic patterns of electrical stimulation for prosthetic sensation". In: *Journal of Neural Engineering* 17.4 (2020), p. 046045.

[76] Maria C. Dadarlat, Joseph E. O'Doherty, and Philip N. Sabes. "A learning-based approach to artificial sensory feedback leads to optimal integration". In: *Nature Neuroscience* 18.1 (2015), pp. 138–144.

[77] G. Risso et al. "Optimal integration of intraneural somatosensory feedback with visual information: a single-case study". In: *Scientific Reports* 9.1 (2019), pp. 1–10.

[78] Ivana Cuberovic et al. "Learning of Artificial Sensation Through Long-Term Home Use of a Sensory-Enabled Prosthesis". In: *Frontiers in Neuroscience* 13.August (2019), pp. 1–24.

[79] Marius Pachitariu et al. *Suite2p: beyond 10,000 neurons with standard two-photon microscopy.* en. preprint. Neuroscience, June 2016.

Table S 1: The shape of the data (Data shape), the shape of the projected data on principal component space (PC projection shape), the obtained significant component (Significant component), and the cumulative proportion of variance explained by the significant component (Variance explained) of the anesthetized mice. num_trial: the number of trials; num_neuron: the number of neurons; len_seq: the length of the concatenated sequence; num_sample: the number of sample used for principal component analysis; num_pc: the total number of the principal components.

Data type	Animal name	Data shape	PC projection shape	Significant component	Variance explained
Anesthetized mouse, Average	-	(num_trial, num_neuron)	(num_sample, num_pc)	-	
	Mouse1	(57, 1719)	(57, 57)	11	0.33
	Mouse2	(53, 901)	(53, 53)	4	0.18
	Mouse3	(60, 1773)	(60, 60)	9	0.34
	Mouse4	(60, 2229)	(60, 60)	16	0.41
	Mouse5	(60, 1950)	(60, 60)	10	0.32
	Mouse6	(60, 1191)	(60, 60)	6	0.24
	Mouse7	(60, 528)	(60, 60)	4	0.26
	Mouse8	(60, 1302)	(60, 60)	2	0.23
Anesthetized mouse, Concat	-	(len_seq, num_neuron)	(num_sample, num_pc)	-	
	Mouse1	(617, 1719)	(617, 617)	55	0.58
	Mouse2	(555, 901)	(555, 555)	49	0.59
	Mouse3	(829, 1773)	(829, 829)	57	0.61
	Mouse4	(421, 2229)	(421, 421)	57	0.62
	Mouse5	(723, 1950)	(723, 723)	60	0.60
	Mouse6	(688, 1191)	(688, 688)	58	0.60
	Mouse7	(720, 528)	(720, 528)	50	0.63
	Mouse8	(677, 1302)	(677, 677)	55	0.63

Table S 2: The shape of the data (Data shape), the shape of the projected data on principal component space (PC projection shape), the obtained significant component (Significant component), and the cumulative proportion of variance explained by the significant component (Variance explained) of the awake mice. num_trial: the number of trials; num_neuron: the number of neurons; len_seq: the length of the concatenated sequence; num_sample: the number of sample used for principal component analysis; num_pc: the total number of the principal components.

Data type	Animal name	Data shape	PC projection shape	Significant component	Variance explained
Awake mouse, Average	-	(num_trial, num_neuron)	(num_sample, num_pc)	-	
	b0039_210525dff	(94, 102)	(94, 94)	2	0.16
	c0008_201120dff	(126, 123)	(126, 123)	3	0.33
	c0010_201113dff	(106, 117)	(106, 106)	7	0.37
	c0021_210310dff	(245, 79)	(245, 79)	3	0.23
	d0008_201124dff	(165, 123)	(165, 123)	6	0.33
	d0010_201113dff	(100, 88)	(100, 88)	5	0.36
	f0010_201120dff	(86, 96)	(86, 86)	2	0.27
	m0010_201211dff	(121, 93)	(121, 93)	7	0.34
Awake mouse, Concat	-	(len_seq, num_neuron)	(num_sample, num_pc)	-	
	b0039_210525dff	(3196, 102)	(3196, 102)	30	0.56
	c0008_201120dff	(4284, 123)	(4284, 123)	21	0.54
	c0010_201113dff	(3604, 117)	(3604, 117)	29	0.57
	c0021_210310dff	(8330, 79)	(8330, 79)	16	0.45
	d0008_201124dff	(5610, 123)	(5610, 123)	30	0.56
	d0010_201113dff	(3400, 88)	(3400, 88)	20	0.55
	f0010_201120dff	(2924, 96)	(2924, 96)	19	0.55
	m0010_201211dff	(4114, 93)	(4114, 93)	28	0.57

Table S 3: The shape of the data (Data shape), the shape of the projected data on principal component space (PC projection size), the obtained significant component (Significant component), and the cumulative proportion of variance explained by the significant component (Variance explained) of the running mice. len_seq: the length of the whole sequence; num_neuron: the number of neurons; num_sample: the number of sample used for principal component analysis; num_pc: the total number of the principal components.

Data type	Animal name	Data shape	PC projection shape	Significant component	Variance explained
Running mouse	-	(len_seq, num_neuron)	(num_sample, num_pc)	-	
	Mouse1	(9361, 3327)	(9361, 3327)	129	0.36
	Mouse2	(9368, 3479)	(9368, 3479)	209	0.39
	Mouse3	(9264, 2978)	(9264, 2978)	155	0.39
	Mouse4	(9248, 3909)	(9248, 3909)	281	0.49
	Mouse5	(9260, 3452)	(9260, 3452)	224	0.41
	Mouse6	(9249, 2653)	(9249, 2653)	115	0.38
	Mouse7	(9254, 3576)	(9254, 3576)	285	0.45
	Mouse8	(9250, 3314)	(9250, 3314)	204	0.43

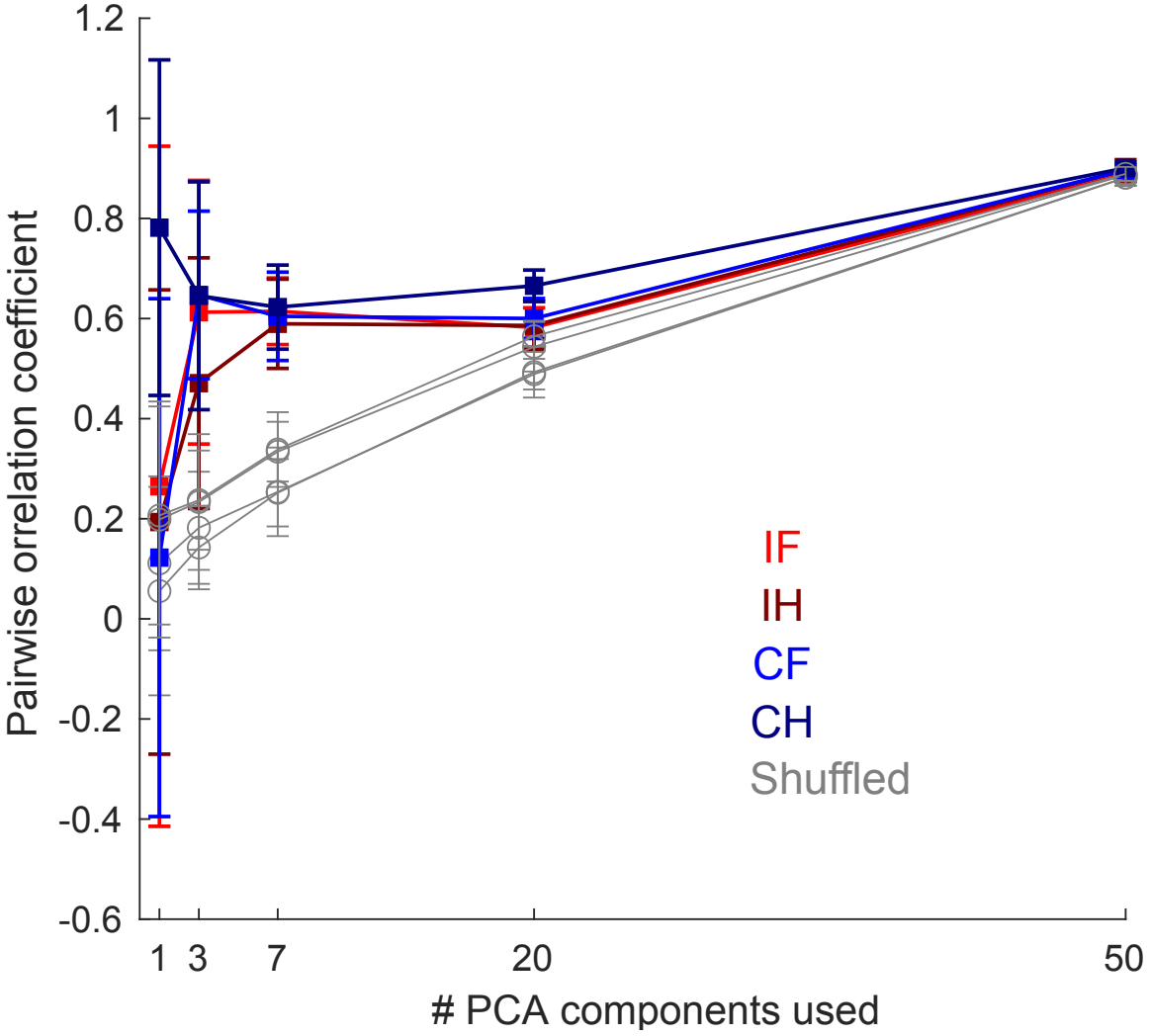

Figure S 1: Correlations between aligned neural trajectories as a function of the number of principal components used for alignment.

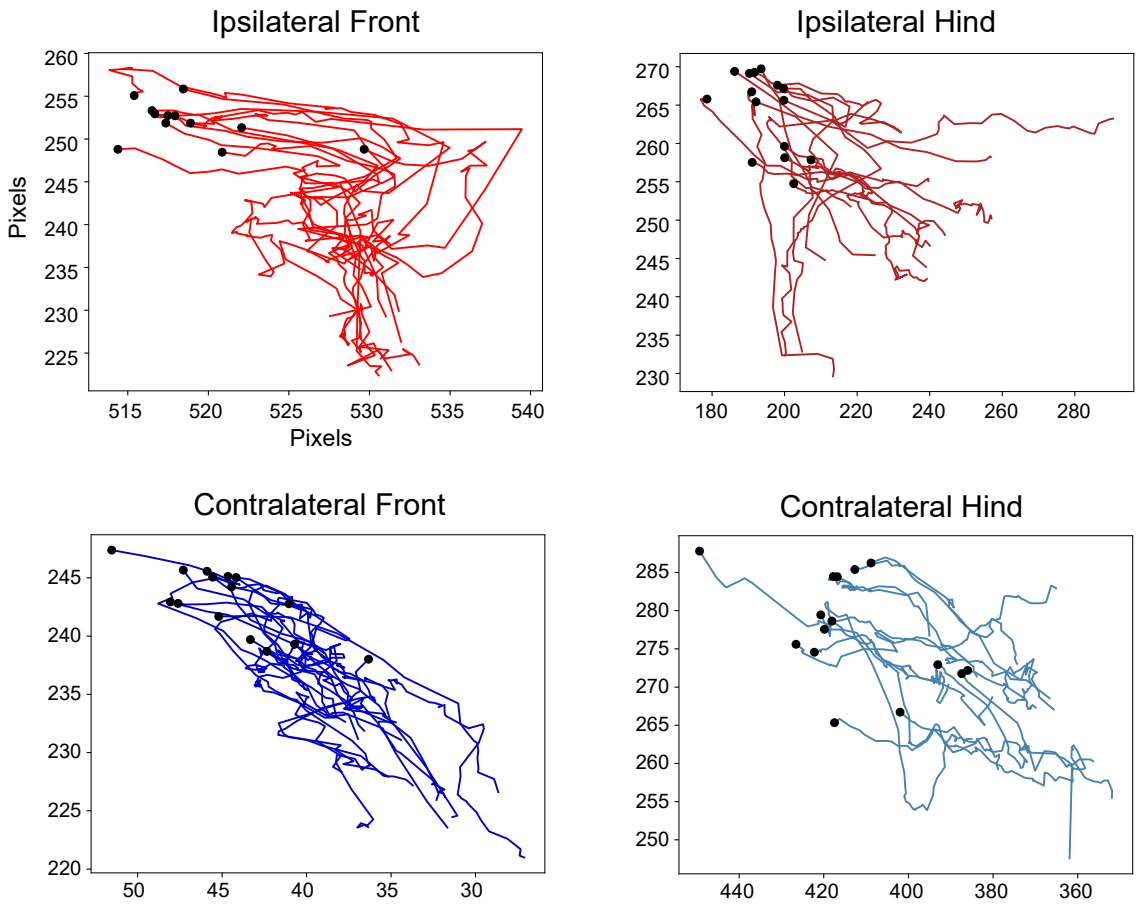

Figure S 2: Trajectories of limb end points of Mouse 1 in video frames with the size of 540 × 400 in anesthetized mouse experiment. Black points show the initial points of trials.

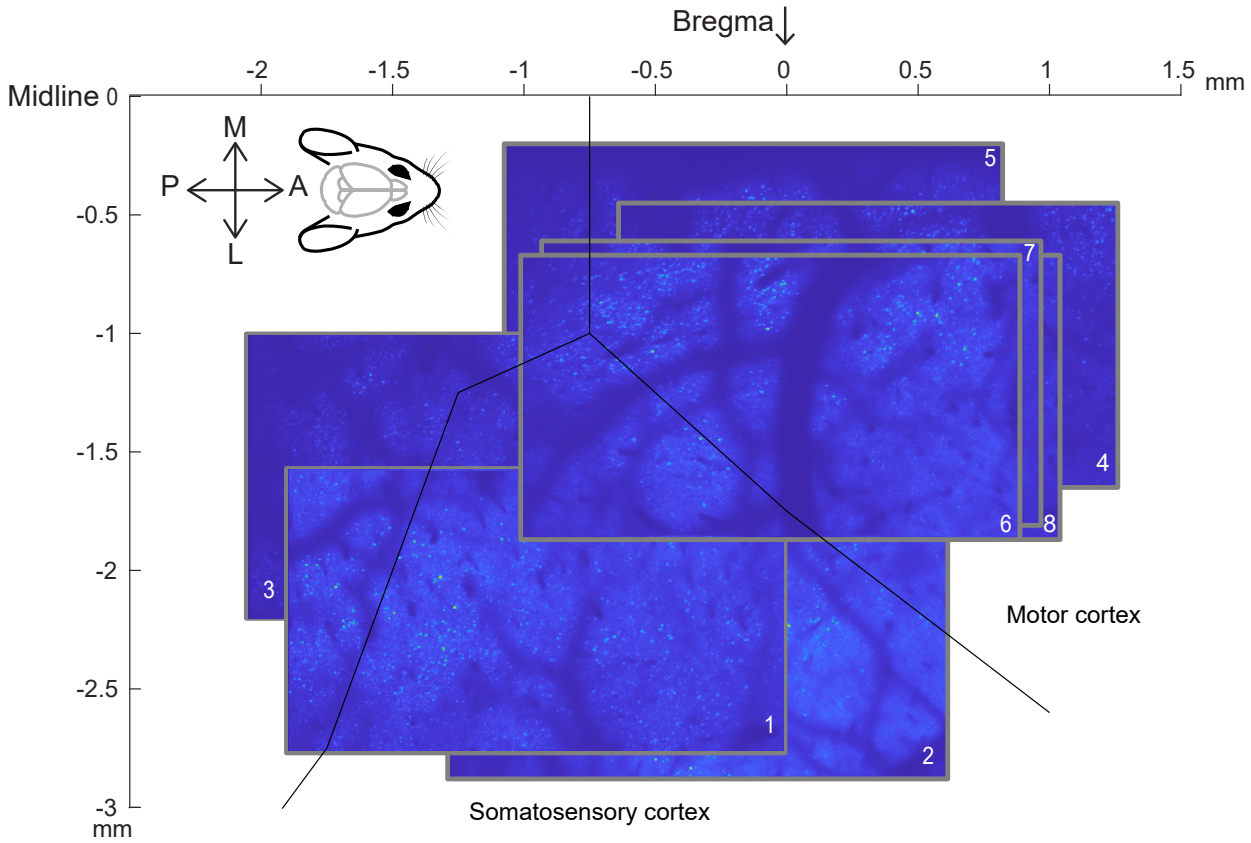

Figure S 3: Imaging windows for anesthetized mice (numbered as in the main text and figures, e.g. Mouse 1). The black line denotes putative anatomical demarcations of somatosensory and motor cortices (**Krumin2018**).